Shaoxiong Zhang, MD, PhD
Jianming Cai, MD, PhD
Ying Luo, PhD
Chao Han, PhD
Nayak L. Polissar, PhD
Thomas S. Hatsukami, MD
Chun Yuan, PhD

Author contributions:
Guarantor of integrity of entire study, S.Z.; study concepts, S.Z., J.C., C.H.; study design, S.Z., J.C., Y.L.; literature research, S.Z.; clinical studies, T.S.H.; experimental studies, S.Z., J.C.; data acquisition, S.Z., J.C.; data analysis/interpretation, S.Z., Y.L., N.L.P.; statistical analysis, S.Z., N.L.P.; manuscript preparation, S.Z., C.H.; manuscript definition of intellectual content, S.Z., C.H., C,Y.; manuscript editing, S.Z.; manuscript revision/review, N.L.P., C.Y.; manuscript final version approval, T.S.H., C.Y.

Measurement of Carotid Wall Volume and Maximum Area with Contrast-enhanced 3D MR Imaging: Initial Observations[1]

PURPOSE: To investigate whether postcontrast three-dimensional (3D) magnetic resonance (MR) imaging would yield more accurate measurement of carotid artery wall volume and maximum wall area, which are both measures of plaque burden, than precontrast 3D MR imaging.

MATERIALS AND METHODS: Eleven consecutive patients scheduled to undergo carotid endarterectomy were recruited for the study. A 3D fast gradient-recalled-echo sequence was applied to acquire both precontrast and postcontrast images of the carotid artery wall. The same sequence was used to image the ex vivo excised plaque as a reference for measurement of carotid wall volume and maximum wall area.

RESULTS: The mean difference in maximum wall area between the precontrast in vivo measurements and the ex vivo measurements (mean ± SD, 18.22 mm^2 ± 15.61) was significantly larger than that between the postcontrast in vivo measurements and the ex vivo measurements (12.33 mm^2 ± 14.49) (P = .02). The difference in wall volume between the precontrast in vivo measurements and the ex vivo measurements (41.81 mm^3 ± 36.51) was larger than that between the postcontrast in vivo measurements and the ex vivo measurements (32.73 mm^3 ± 35.00) (P = .004). Postcontrast images yielded better correlation with ex vivo images than did precontrast images, in both carotid luminal area (R = 0.88 for postcontrast images, R = 0.80 for precontrast images) and outer wall boundary area (R = 0.79 for postcontrast images, R = 0.71 for precontrast images) measurements.

CONCLUSION: Postcontrast 3D MR imaging may be useful in the measurement of carotid artery plaque burden.

Atherosclerotic disease, which is the leading cause of death in the United States, is a disease of the vessel wall that eventually causes luminal stenosis. The severity of atherosclerosis may be determined by assessing both luminal stenosis and lesion morphology. Assessment of luminal stenosis alone is limited in predicting the clinical outcome and the natural history of the disease. It is known that during the early stages of atherosclerotic plaque growth, the vessel may remodel and accommodate plaque growth without compromising luminal size (1). Findings of clinical trials have shown that in human carotid arteries, luminal stenosis is a limited indicator of atherosclerotic plaque vulnerability, enabling prediction of one of four strokes in symptomatic patients (2) and only one of 10 strokes in asymptomatic patients (3). Plaque burden, which is represented by plaque volume and maximum wall area (MWA), as a direct measure of the lesion itself may have substantial usefulness in the assessment of atherosclerosis.

Magnetic resonance (MR) imaging is a noninvasive method that demonstrates excellent soft-tissue contrast and sensitivity to flow. It has advantages over other modalities in depicting the arterial wall and may play a unique role in monitoring atherosclerotic lesion

progression and regression. Previous work has demonstrated the ability of MR imaging to characterize the composition of human atherosclerotic plaques, both ex vivo and in vivo (4–6). Two-dimensional black-blood high-spatial-resolution MR imaging techniques with multiple contrast weightings have been shown to be useful in the characterization of atherosclerotic tissue (4,6,7). Black-blood techniques have also been used in plaque area measurement (8–13). While bright-blood MR techniques have been widely used in identifying vessel lumen stenosis, they have only recently been applied to plaque characterization (6,14), especially the identification of fibrous caps (14).

Among bright-blood MR imaging techniques, three-dimensional (3D) time-of-flight and 3D gradient-recalled-echo (GRE) techniques may be of particular use because of their inherent high-spatial-resolution data acquisition and their usefulness in both lumen and wall depiction (15,16). Study findings have shown that gadolinium-based contrast agents can penetrate into the arterial wall, including the adventitia layer of the artery, which marks the outer wall boundary (17,18). Thus, the combination of contrast enhancement and 3D data acquisition may provide a very useful tool for evaluating plaque area and volume. The purpose of this study was to investigate whether 3D MR imaging performed after contrast material administration would yield more accurate measurement of carotid wall volume and MWA (both are measures of plaque burden) than 3D MR imaging performed before contrast material administration.

MATERIALS AND METHODS

Patient Population

Between January and November 2000, 11 consecutive patients (mean age ± SD, 61 years ± 9) scheduled to undergo carotid endarterectomy at the University of Washington Medical Center and the Puget Sound Veteran's Affairs Medical Center were recruited for the study. Informed consent for the MR imaging was obtained from all patients. The consent forms and protocol were approved by each facility's institutional review board. Each patient underwent MR imaging of the extracranial carotid arteries before surgery.

MR Examination

All MR imaging examinations were conducted with a 1.5-T whole-body imager (Signa Horizon Echospeed, version 5.8; GE Medical Systems, Milwaukee, Wis). Four-element custom-built phased-array coils (two elements on the right side of the neck and two on the left) were used to improve the signal-to-noise performance of the imager (19). Studies of the performance of these phased-array coils, which have overall dimensions of 6.4 × 10.8 cm, demonstrated a 37% improvement in the signal-to-noise ratio compared with the signal-to-noise ratio of commercially available 3-inch-diameter (7.6 cm) surface coils (19).

A 3D fast GRE sequence was applied to acquire both precontrast and postcontrast images of the carotid artery centered at the bifurcation of the side of surgery (within 5–10 minutes after injection of contrast agent). Imaging parameters were 9.8/2.4 (repetition time msec/echo time msec) with a 13-cm field of view, 2-mm section thickness, matrix of 256 × 256, two signals acquired, and 20° flip angle.

A total dose of 20 mL of gadodiamide (Omniscan; Nycomed Amersham, Oslo, Norway) was injected at a rate of 2 mL/sec. To reduce the signal from subcutaneous fat and to avoid chemical shift artifacts, a fat-saturation technique was applied in 3D fast GRE sequences. A zero-filled Fourier transform was used to create voxels of 0.25 × 0.25 × 1 mm for 3D fast GRE imaging. All in vivo MR imaging examinations were performed less than 3 days before surgery. During surgery, the atherosclerotic plaque was removed en bloc and placed in saline at 4°C.

A 3D fast GRE imaging study was conducted ex vivo on the excised plaque as a reference for carotid wall volume measurement. The imaging parameters were identical to those used in vivo with the exception of a section thickness of 1 mm and a field of view of 8 cm. MR imaging of this surgical specimen was performed at body temperature (37°C) within 4 hours of the surgery while the specimen was submerged in saline.

Measurement of Wall Volume and MWA

Carotid luminal and outer wall boundaries were measured by using a custom-designed program, the Quantitative Vascular Analysis Tool, or QVAT (9,12), which was developed with Interactive Data Language. For in vivo images, the outer vessel wall boundary was defined as the vessel wall–soft-tissue interface; for ex vivo images, the outer vessel wall boundary was defined as the vessel wall–background saline interface.

To measure the cross-sectional area of the carotid artery, the operator manually placed initial points near the lumen and outer wall boundaries. Boundaries were then searched by the Quantitative Vascular Analysis Tool program by using the Snake algorithm (9,12), and the area was automatically calculated. Wall area was defined as the area encircled by subtracting the luminal area from the outer wall boundary area. Two reviewers conducted a blinded review of in vivo and ex vivo images. One author measured in vivo images, and the other author measured ex vivo images. In vivo and ex vivo images were evaluated independently to avoid potential bias.

Definition of Wall Volume and MWA

Wall volume was calculated by multiplying the sum of cross-sectional areas and the section thickness. In each case, 10 locations centered at carotid bifurcation were used for wall volume measurement. MWA was defined as the largest area among the common carotid, bifurcation, and internal carotid artery wall.

Data Analysis

The location of the carotid bifurcation was determined with both in vivo and ex vivo images and was defined as the location of conversion from a single lumen to dual lumina. Once this location was defined, all other image locations were referenced to it in millimeters: Distal locations were given positive values, and proximal locations were given negative values. The in vivo and ex vivo images were then matched according to their locations.

Precontrast and postcontrast wall volume and MWA measurements were compared by using ex vivo images as reference. The mean absolute differences in wall volume and MWA of precontrast or postcontrast and ex vivo values were calculated and assessed by using the Student paired t test. A value of $P < .05$ was considered to indicate a statistically significant difference. Cross-sectional areas of the carotid artery lumen and outer wall boundary on precontrast and postcontrast in vivo images were compared with those on ex vivo images. The Pearson correlation coefficient was used as a descriptive measure of the strength of association between measurements of in vivo and ex vivo images.

RESULTS

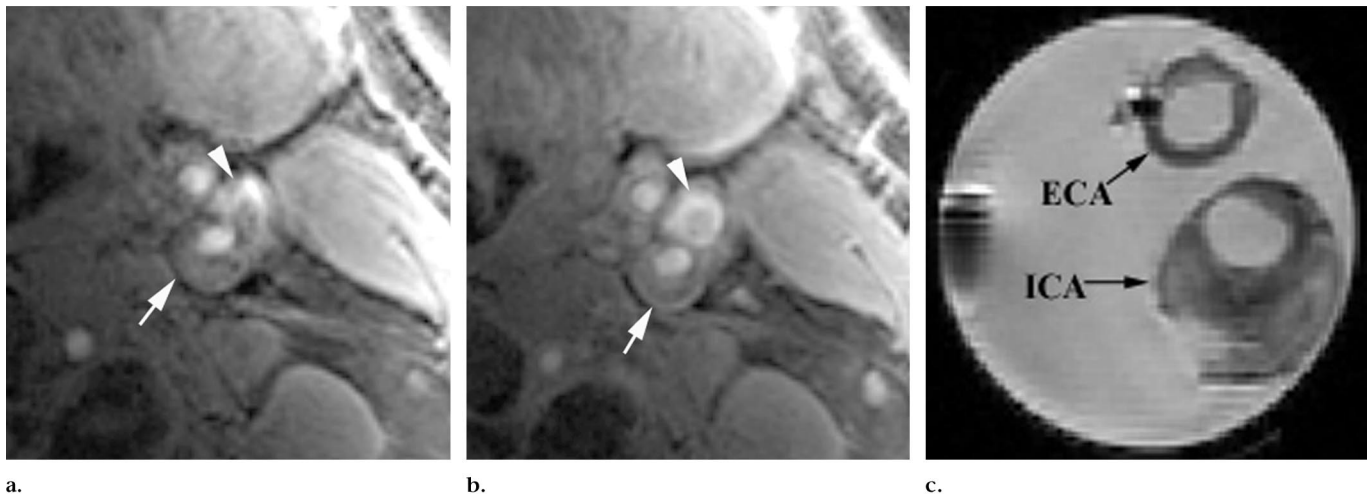A total of 110 images (10 locations × 11 patients) were available for this study. In

Figure 1. Three-dimensional fast GRE MR images of carotid artery. **(a)** On precontrast image, outer wall boundary of internal carotid artery (arrow) and jugular vein (arrowhead) are unclear. **(b)** On postcontrast image, outer wall boundary of internal carotid artery (arrow) is clearly delineated as a bright rim. Jugular vein (arrowhead) is better delineated than on **a**, with a clear vein-artery interface. Imaging parameters for **a** and **b** are 9.8/2.4 with a 13-cm field of view, 2-mm section thickness, matrix of 256 × 256, two signals acquired, and 20° flip angle. **(c)** Ex vivo image. *ECA* = external carotid artery, *ICA* = internal carotid artery. Imaging parameters are 9.8/2.4 with an 8-cm field of view, 1-mm section thickness, matrix of 256 × 256, two signals acquired, and 20° flip angle.

TABLE 1
Measurement of Carotid Wall Volume and MWA with ex Vivo and in Vivo Imaging

Measurement	Ex Vivo Imaging	In Vivo Imaging	
		Precontrast	Postcontrast
Wall volume (mm^3)	699.11 ± 317.40	740.93 ± 294.93	731.79 ± 297.28
MWA (mm^2)	74.83 ± 21.73	93.05 ± 21.83	87.15 ± 20.38

TABLE 2
Comparison of Precontrast Minus ex Vivo and Postcontrast Minus ex Vivo Measurements of Carotid Wall Volume and MWA

Measurement	Precontrast − ex Vivo Measurements	Postcontrast − ex Vivo Measurements	P Value
Wall volume (mm^3)	41.81 ± 36.51	32.73 ± 35.00	.004
MWA (mm^2)	18.22 ± 15.61	12.33 ± 14.49	.02

Note.—Data are mean ± SD of absolute differences.

all cases, the carotid wall volume and MWA on both precontrast and postcontrast in vivo images were always larger than those on ex vivo images. The smaller ex vivo wall volume and MWA were expected, since the ex vivo measurement was of excised plaque, which includes the atherosclerotic intima and part of the media. The in vivo measurement, however, was of the entire artery wall (intima, media, and adventitia).

As shown in Figure 1, the carotid artery outer wall and jugular vein boundaries are better delineated on postcontrast images than on precontrast images because of the substantial enhancement of the adventitia layer of the artery. On the basis of visual review, nine of the ll patients had improved delineation of the outer wall boundary on postcontrast images and two showed no difference. On postcontrast 3D fast GRE images, the enhancement of the outer wall boundary of the carotid artery appeared as full or partial circumference. The boundary between the carotid artery and the jugular vein was better delineated in comparison to precontrast 3D fast GRE images (Fig 1). In addition, seven patients had better luminal delineation on postcontrast images than on precontrast images. In all patients with clear postcontrast delineation of outer wall and luminal boundaries, measurements obtained from postcontrast images yielded closer wall volume and MWA results compared with ex vivo images than did measurement obtained from corresponding precontrast images compared with ex vivo images.

Measurement of Wall Volume and MWA

The mean measurements of carotid wall volume and MWA on precontrast and postcontrast in vivo images and on ex vivo images are shown in Table 1. There was a significant difference between precontrast and postcontrast MWA measurements; as shown in Table 2, the mean absolute difference in MWA between precontrast and ex vivo measurements was significantly larger than that between postcontrast and ex vivo measurements (*P* = .02). The mean absolute difference in wall volume between precontrast and ex vivo measurements was also significantly larger than that between postcontrast and ex vivo measurements, which is 41.81 mm^3 and 32.73 mm^3, respectively (*P* = .004). Both of these results show that postcontrast area and volume measurements have closer association with the ex vivo measurements.

Measurement and Visualization of Carotid Artery Lumen and Outer Wall Boundary

On the basis of analysis of all individual cross-sectional images, both lumen
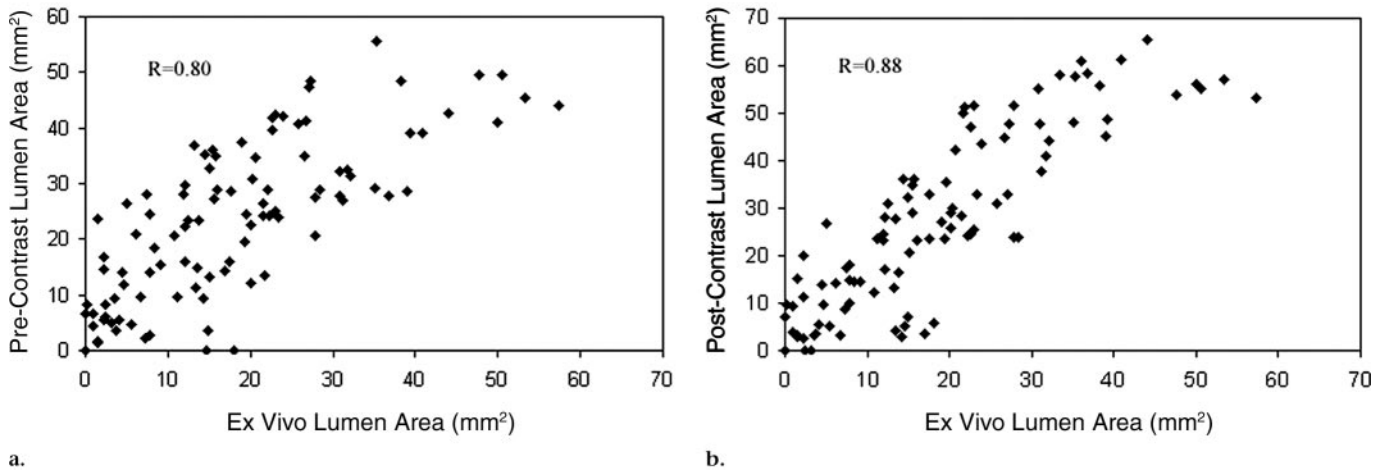
Figure 2. (a, b) Graphs show relationship between luminal area measured on in vivo MR images and on ex vivo MR images. Postcontrast 3D fast GRE images (**b**, R = 0.88) yielded better correlation with ex vivo 3D fast GRE images than did precontrast images (**a**, R = 0.80) in measurement of carotid luminal area. Zero measurements in some cases are due to totally occluded lumina.
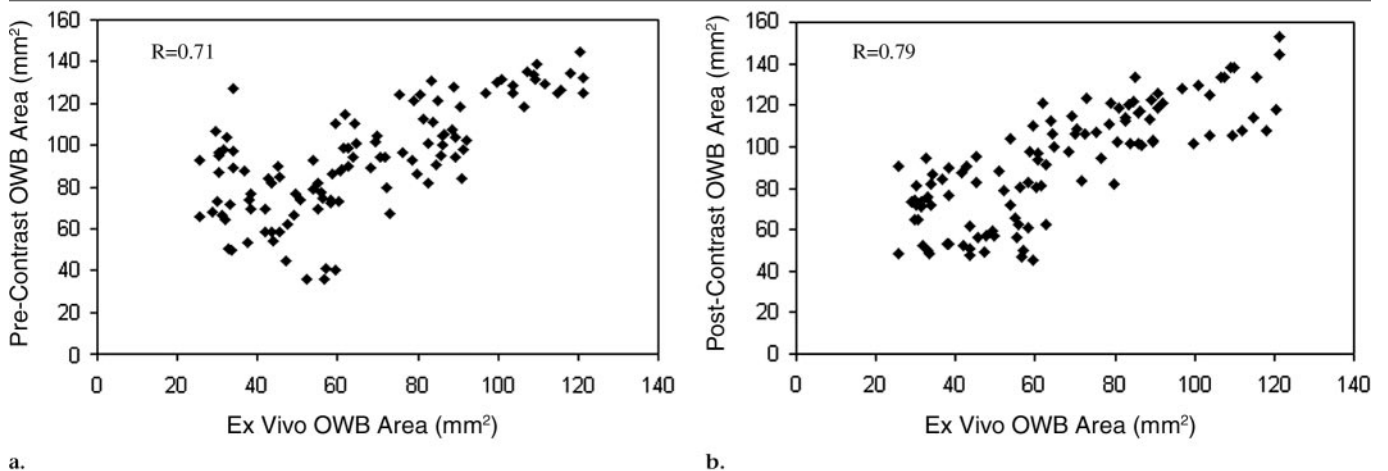

Figure 3. (a, b) Graphs show relationship between outer wall boundary (*OWB*) of carotid artery measured on in vivo MR images and on ex vivo MR images. Postcontrast 3D fast GRE images (**b**, R = 0.79) yielded better correlation with ex vivo 3D fast GRE images than did precontrast images (**a**, R = 0.71).

and outer wall boundary areas on postcontrast 3D fast GRE images correlated better with ex vivo images than did precontrast images (Figs 2 and 3).

DISCUSSION

Black-blood two-dimensional MR techniques have played important roles in the characterization of atherosclerotic lesions and have been also used for quantitative analysis of carotid artery disease (4–6,8–13). However, two-dimensional black-blood MR protocols usually have a relatively long imaging time, which will challenge a patient's tolerance and may introduce motion artifacts. Three-dimensional MR imaging offers better resolu-

tion in the section-selected direction and has a higher signal-to-noise ratio than does two-dimensional imaging. By using a repetition time as short as 9.8 msec, the 32-section 3D fast GRE images in this study can be achieved within 2 minutes. Furthermore, 3D techniques eliminate the misregistration between sections that may occur in two-dimensional images, and 3D images are able to provide isotropic voxel volumes that can be used to obtain reformatted images in any plane desirable (20). In addition, as a bright-blood technique, 3D fast GRE imaging is capable of minimizing the influence of underlying calcification on plaque burden measurement that may affect accurate luminal definition on black-blood

images. This is because calcium on the luminal surface appears dark and the lumen appears bright on 3D fast GRE images, while both calcium and lumen appear dark on black-blood MR images.

Currently, carotid area is usually measured on precontrast MR images (8–13). Our study findings show that postcontrast 3D fast GRE imaging yields better measurements for both plaque volume and MWA than does precontrast 3D fast GRE imaging. This result suggests that 3D bright-blood technique may be useful in the quantitation of plaque volume.

There have been reports that the bright rim of the vessel wall can be identified with postcontrast MR imaging (17,21,22). Aoki et al (17,21) and Lin et al (22) reported that

the outer wall can have atherosclerosis-like enhancement. As we found, on postcontrast MR images the outer wall boundary is more clearly delineated, which directly contributes to better measurement of the area of the carotid artery. In our study, visible enhancement of the outer wall boundary on postcontrast images was identified in nine (82%) of 11 patients, while two (18%) of 11 patients showed no visible changes. Such minimal enhancement may be due to images that were not acquired at the peak perfusion time of the contrast agent and to substantial plaque enhancement that made the enhancement of the outer wall boundary less obvious.

The main limitation of precontrast 3D bright-blood MR imaging is signal loss caused by *(a)* saturation of slow flow in normal and disease conditions and *(b)* dephasing due to complex or turbulent flow, which is particularly problematic in patients with severe stenosis (23). If a T1-shortening contrast agent is injected, however, postcontrast 3D MR imaging could eliminate the signal loss in lumen that is caused by saturation of slow flow and turbulent flow, especially at the carotid bifurcation. Thus, better luminal delineation would be achieved on postcontrast images. Without contrast enhancement, the difficulty in recognizing the boundary between the carotid artery and jugular vein could introduce error in measurement. In general, postcontrast 3D MR imaging provides better definition than precontrast imaging of carotid artery lumen and outer wall boundary, as well as the carotid-jugular vein boundaries, all of which affect the accuracy of carotid artery wall volume and MWA measurement.

Previous studies in which MWA was measured on two-dimensional black-blood images demonstrated a mean difference (value from in vivo image minus value from ex vivo image $\pm$ SD) of 13.1 mm^2 $\pm$ 6.5 for T1-weighted images and of 14.1 mm^2 $\pm$ 11.7 for intermediate-weighted images (11). MWA measurement on postcontrast 3D fast GRE images, in comparison to two-dimensional black-blood images, yielded comparable or slightly better results with a mean difference of 12.33 mm^2 $\pm$ 14.49, while the difference of the measurement was increased on precontrast 3D fast GRE images with a mean difference of 18.22 mm^2 $\pm$ 15.61 (Table 2). These results clearly demonstrate the importance of accurate demarcation of the outer wall boundary on 3D fast GRE images as a result of contrast enhancement. A recent publication demonstrated the usefulness of postcontrast high-spatial-resolution MR imaging in the characterization of atherosclerotic tissue (18). Thus, postcontrast 3D fast GRE imaging may be particularly useful in providing information on both the evaluation of plaque burden and the characterization of atherosclerotic tissue. This may aid in the identification of neovascularization and in the differentiation of necrotic core from fibrous tissue.

Vessel stenosis and MWA measurements from ex vivo imaging, which is used as the reference standard, have been reported previously (11,24). The technique, which was described by Pan and co-workers (24), showed that there was little change in luminal size between in vivo and ex vivo studies at the site of atherosclerosis. In our study, the ex vivo measurements were conducted within 4 hours of surgery while the specimen was at body temperature. We expect there was little shrinkage or other alteration to the plaque specimen in this time. It is expected that wall volume and MWA measurements from in vivo images are larger than those from ex vivo images in this study. During surgery, only plaque is removed from the vessel wall, so specimens are truly parts of the vessel wall. Carotid wall in vivo measurements, however, include media and adventitia, as well. To our knowledge, there has been no report on the ability of MR imaging to allow differentiation of the three layers of vessel wall—intima, media, and adventitia—in vivo. If this ability is achieved in the future, direct comparison will be possible between in vivo and ex vivo specimens of plaque burden. A study on comparison of presurgical, postsurgical, and ex vivo specimens may give us better understanding on this issue.

In conclusion, our results demonstrate that postcontrast 3D fast GRE MR imaging is superior to precontrast MR imaging in quantifying plaque burden, as assessed with MWA and plaque volume. Contrast enhancement provides better delineation of the lumen and outer artery wall boundaries and less flow artifact from slow flow, which results in closer agreement between in vivo measurements and the standard of reference, ex vivo measurements. Measurement of plaque burden with MR imaging will have important applications in studies in which the relationship between lesion size and clinical outcome is examined and in clinical trials in which plaque regression in response to therapeutic intervention is examined.

References
1. Glagov S, Weisenberg E, Zarins CK, Stankunavicius R, Kolettis GJ. Compensatory enlargement of human atherosclerotic coronary arteries. N Engl J Med 1987; 316:1371–1375.
2. North American Symptomatic Carotid Endarterectomy Trial Collaborators. Beneficial effect of carotid endarterectomy in symptomatic patients with high-grade stenosis. N Engl J Med 1991; 325:445–453.
3. Executive Committee for Asymptomatic Carotid Atherosclerosis Study. Endarterectomy for asymptomatic carotid artery stenosis. JAMA 1995; 273:1421–1428.
4. Shinnar M, Fallon JT, Wehrli S, et al. The diagnostic accuracy of ex vivo MRI for human atherosclerotic plaque characterization. Arterioscl Thromb Vasc Biol 1999; 19:2756–2761.
5. Toussaint JF, LaMuraglia GM, Southern JF, et al. Magnetic resonance images lipid, fibrous, calcified, hemorrhagic and thrombotic components of human atherosclerosis in vivo. Circulation 1996; 94:932–938.
6. Yuan C, Mitsumori LM, Ferguson MS, et al. In vivo accuracy of multispectral magnetic resonance imaging for identifying lipid-rich necrotic cores and intraplaque hemorrhage in advanced human carotid plaques. Circulation 2001; 104:2051–2056.
7. Yuan C, Mitsumori LM, Beach KW, Maravilla KR. Carotid atherosclerotic plaque: noninvasive MR characterization and identification of vulnerable lesions. Radiology 2001; 221:285–299.
8. Fayad ZA, Nahar T, Fallon JT, et al. In vivo magnetic resonance evaluation of atherosclerotic plaques in the human thoracic aorta. Circulation 2000; 101:2503–2509.
9. Zhang S, Hatsukami TS, Polissar NL, Han C, Yuan C. Comparison of carotid vessel wall area measurements using three different contrast-weighted black blood MR imaging techniques. Magn Reson Imaging 2001; 19:795–802.
10. Fayad ZA, Fuster V, Fallon JT, et al. Noninvasive in vivo human coronary artery lumen and wall imaging using black-blood magnetic resonance imaging. Circulation 2000; 102:506–510.
11. Yuan C, Beach KN, Smith LH, Hatsukami TH. Measurement of atherosclerotic carotid plaque size in vivo using high resolution MRI. Circulation 1998; 98:2666–2671.
12. Yuan C, Lin E, Millard J, Hwang JN. Closed contour edge detection of blood vessel lumen and outer wall boundaries in black-blood MR images. Magn Reson Imaging 1999; 17:257–266.
13. Kang X, Polissar NL, Han C, Lin E, Yuan C. Analysis of the measurement precision of arterial lumen and wall areas using high-resolution MRI. Magn Reson Med 2000; 44:968–972.
14. Hatsukami TS, Ross R, Polissar NL, Yuan C. Visualization of fibrous cap thickness and rupture in human atherosclerotic carotid plaque in vivo with high-resolution

magnetic resonance imaging. Circulation 2000; 102:959–964.

15. Luk-Pat GT, Gold GE, Olcott EW, et al. High-resolution three-dimensional in vivo imaging of atherosclerotic plaque. Magn Reson Med 1999; 42:762–777.

16. Sardanelli F, Zandrino F, Parodi RC, Caro GD. MR angiography of internal carotid arteries: breath-hold Gd-enhanced 3D fast imaging with steady-state precession versus unenhanced 2D and 3D TOF techniques. J Comput Assist Tomogr 1999; 23:208–215.

17. Aoki S, Nakajima H, Kumagai H, Araki T. Dynamic contrast-enhanced MR angiography and MR imaging of the carotid artery: high resolution sequences in different acquisition planes. AJNR Am J Neuroradiol 2000; 21:381–385.

18. Yuan C, Kerwin WS, Ferguson MS, et al. Contrast-enhanced high resolution MRI for atherosclerotic carotid artery tissue characterization. J Magn Reson Imaging 2002; 15:62–67.

19. Hayes CE, Mathis CM, Yuan C. Surface coil phased arrays for high resolution imaging of the carotid arteries. J Magn Reson Imaging 1996; 1:109–112.

20. Barger AV, Grist TM, Block WF, Mistretta CA. Single breath-hold 3D contrast-enhanced method for assessment of cardiac function. Magn Reson Med 2000; 44:821–824.

21. Aoki S, Aoki K, Ohsawa S, Nakajima H, Kumagai H, Araki T. Dynamic MR imaging of the carotid wall. J Magn Reson Imaging 1999; 9:420–427.

22. Lin W, Abendschein DR, Haccke EM. Contrast-enhanced magnetic resonance angiography of carotid arterial wall in pigs. J Magn Reson Imaging 1997; 7:183–190.

23. Korosec FR, Turski PA, Carroll TJ, Mistretta CA, Grist TM. Contrast-enhanced MR angiography of the carotid bifurcation. J Magn Reson Imaging 1999; 10:317–325.

24. Pan XM, Saloner D, Reilly LM, et al. Assessment of carotid artery stenosis by ultrasonography, conventional angiography, and magnetic resonance angiography: correlation with ex vivo measurement of plaque stenosis. J Vasc Surg 1995; 21:82–88.